Korean J. Chem. Eng., 35(1), 153-163 (2018)
DOI: 10.1007/s11814-017-0254-3

pISSN: 0256-1115
eISSN: 1975-7220

Adsorptive removal of fluoride from water samples using *Azospirillum* biofertilizer and lignite

Kavita Kulkarni*,*,†, Gajanan M. Bhogale*, and Rujuta Nalawade****

*Shri J. J. T. University, Rajasthan 333001, India
**Department of Environmental Science, Savitribai Phule Pune University, Pune 411007, India
***Department of Chemical Engineering, Bharati Vidyapeeth University College of Engineering, Pune 411043, India
(*Received 11 June 2017 • accepted 18 September 2017*)

Abstract−The present study involves a comparison of *Azospirillum* biofertilizer and lignite for removal of fluoride from aqueous solution. Batch experiments were performed to remove fluoride by the use of *Azospirillum* biofertilizer and lignite. Fluoride adsorption capacity was found by varying different parameters such as adsorbent dose, pH, initial concentration, temperature and contact time. The adsorption capacity for fluoride by using *Azospirillum* biofertilizer was 0.456 mg/g and for lignite 0.16 mg/g. Pseudo-second-order kinetic model best fit the experimental data. Field water samples were tested for fluoride removal by *Azospirillum* biofertilizer and lignite. The fluoride concentration was reduced to the permissible limit.

Keywords: *Azospirillum* Biofertilizer, Lignite, Fluoride, Adsorption, Removal Efficiency

INTRODUCTION

The amount of high fluoride concentration beyond acceptable limit in ground water is a problem faced by many countries mainly India, Sri Lanka, Pakistan, China and parts of East Africa.

Drinking water is the major source of fluoride intake. The World health organization has specified the acceptable limit of fluoride as 1.5 ppm [1,2]. Below 1 mg/*l* of fluoride is beneficial to dental caries, but above 1.5 mg/*l* it can cause dental and skeletal fluorosis. Positively charged calcium ions present in teeth and bones attract fluoride ions due to its strong electro negativity, which causes various types of fluorosis [3-5]. Excess of fluoride may cause neurological disorders. Consumption of fluoride over the prescribed limit by WHO can cause diseases like syndrome, thyroid diseases and cancer [6]. For environmental conservation and human health, the removal of fluoride ion is important. Various defluoridation technologies are used, such as ion exchange [7-11], activated alumina [12-15], membrane filtration [16,17], chemical precipitation [18,19], adsorption [20,21]. Among these, adsorption seems to be the best due to lower operating costs and simple operation. Different adsorbents have been demonstrated for defluoridation, like alumina and aluminum, activated alumina, iron based adsorbents, calcium based adsorbents, metal oxides, biosorbents, natural materials, building materials, nano adsorbents and industrial waste adsorbents. Conventional adsorbents are used to remove fluoride but these are expensive and have some limitations. Because of the increase in environmental awareness, different biosorbents like waste from agricultural material, natural materials and microorganisms are the alternative adsorbents used for defluoridation. Biosorbents are cheap, which are present in large quantities and do not require an expensive regeneration process. The use of biosorbents or biomass from various microbial species, plant based adsorbents has been reported by various researchers [22-30]. Dried tea ash is used as adsorbent for defluoridation. Batch adsorption experiments were performed for different parameters. Fluoride removal is dependent on pH as it changes the charge on the surface of adsorbent. At pH 6.5, the surface has a positive charge and maximum fluoride is adsorbed [31]. Algal biosorbent (Spirogyra IO_2) has been used for defluoridation. Capacity of fluoride removal was 54% [32]. Waste fungal biomass (*Pleurotus Asteratus 1804*) was used for removal of fluoride. The fluoride sorption efficiency was 52% [33]. Bacterium *Acinetobacter* sp. RH_5 was used for defluoridation from ground water collected from Madhabpur and Asanjola, India. Fluoride removal capacity capability was found to be 25.7%. Bacteria give high affinity anion binding compounds which are responsible for removal of fluoride [34]. *Micrococcus luteus* and *Pseudomonas aerugenosa* were used for removal of fluoride. The reduction of fluoride by both the microorganisms after 12 days was 19.8% and 22.1% respectively. Isolates showed ionphores within the cyst which are found to be proficient in fluoride removal [35]. A biomass of *Anabaena fertilissima*, *Chlorococcum humicola*, and green algae, was used for removal of fluoride. The algal biomass, pretreated with Ca^{2+}, was also used for the defluoridation. The sorption was found to be chemisorption. A continuous increase in biosorption of fluoride was observed up to 15 mg/*l* for the biomass [36]. Aquatic microphyte biomass pretreated by Ca^{2+} was used for removal of fluoride. The fluoride removal efficiency was found to be 64.5% at pH 6. Ca^{2+} pretreated biomass showed 0.111 mmol/g fluoride removal efficiency [37]. Two types of activated carbon were pretreated from *Eichhornia crassipes* at 300 °C and 600 °C. Fluoride adsorption capacity was found more on activated carbon prepared at 600 °C (51%-93%). Langmuir adsorption model was followed

†To whom correspondence should be addressed.
E-mail: kavitashreya@gmail.com

by both the carbons. Maximum capacity was found to be 1.54 mg/g. In continuous studies, the breakthrough capacity was 4.4 mg/g [38].

Plants are affected by fluoride contaminated in soil [39]. Fluoride absorbed is carried to the shoots. Depending on the concentration in the cell liquid, it may cause physiological, biochemical and structural damage. Even cell death can occur, depending on the fluoride absorbed [40]. Some plants build up fluoride at higher concentration but do not show signs of toxicity [41], while some species like *Gladiolus* and *Freesia* are extremely responsive to concentration<20 mg/*l* [42,43]. It was found that fluoride concentration was the highest in the vegetables and cereal crops near the vicinity of a brick kiln, followed by the areas dominated by soil, which contains excess salts predominated by sodium chloride [44]. Use of bacteria increases the crop production in large scale [45]. Researchers have reviewed the vast list of microbes and their metal binding capacities [46]. Bacteria may absorb and accumulate cations and anions that are harmful to environment and human health [47]. The surface of microbial cells is rich in functional groups which act as sorption site of chemical species [48]. This beneficial property of bacterial biomass was studied and utilized for removal of fluoride [49].

Biofertilizer contains living cells or latent cells of proficient strains of microbes which assist crop plants to take nutrients by accelerating several microbial processes. These microbial processes help to absorb and digest the nutrients. Such types of microorganisms are immobilized on carrier material to increase the availability of surface area and cell count. The use of perfect carrier material is essential for making a high quality biofertilizer. Lignite and peat soil are used as superior carrier material for preparation of various biofertilizer. Carrier material lignite possesses high organic matter and more moisture holding capacity. Organic material in the soil is enriched by the carbon present in the lignite. Lignite also has property to control the activity of microbes, which causes diseases to plants. It works like an alternative to chemical pesticides [50]. *Azospirillum* is a nitrogen fixing bacteria. About 30 to 50% of nitrogen required for the plant is provided by this microorganism. Auxin and Cytokinin, growth hormones were produced by the *Azospirillum*. Use of *Azospirillum* increases the crop production. *Azospirillum* biofertilizer contains 35% moisture and 63% lignite and 2% *Azospirillum* bacteria. Use of lignite along with *Azospirillum* is accountable for increase in crop production at large scale. *Azospirillum* biofertilizer is used as biofertilizer to increase the crop production.

Batch experiments were performed using *Azospirillum* bacteria, lignite and *Azospirillum* biofertilizer. The fluoride removal efficiency was 17-18% for the *Azospirillum* bacteria. For lignite it increased up to 67%. The combination of *Azospirillum* bacteria and lignite which is *Azospirillum* biofertilizer gave maximum efficiency, 76%. *Azospirillum* biofertilizer and lignite was used as adsorbent in this study for the removal of fluoride. The purpose of using this as adsorbents is that it can serve both as adsorbent for removal of fluoride and as biofertilizer, which will be beneficial for crops. Lignite was used as carrier so it was also tested for removal of fluoride. Researchers have done work on lignite for removal of fluoride [51].

EXPERIMENTAL

1. Adsorbent and its Characterization

Azospirillum biofertilizer was purchased from Agriculture College, M.P.K.V. Rahuri, Pune. 1-2% of *Azospirillum* bacteria were added to carrier material, lignite, to get a cell count of 10^8. Lignite was purchased from a local market. Both the adsorbents were used as is. To determine the morphology and elements present in the adsorbent, scanning electron microscopy and electron dispersive X ray analysis were done using COMP.JEOL, mod, JSM 6360A, respectively. XRD of both adsorbent was done by Bruker Model-D8 Advance.

2. Adsorbate

All used chemicals were of analytical grade and purchased from a local market, Pune, India. 2.21 g of NaF (AR grade) was dissolved in 1,000 ml of double distilled water and used as stock solution for the experiments. Appropriate dilution was done for the desired concentration.

3. Batch Adsorption Study

By using *Azospirillum* biofertilizer and lignite, batch experiments were carried out. Experiments were conducted for different parameters. All the experiments were carried out in a horizontal shaker (Remi Electrotechnik. Ltd. (Model-RS24BL, 220 V, 50 Hz, 10AC). For each experiment, 100 ml of fluoride solution for varied concentration of fluoride like 5, 10, 15, 20 and 25 mg/*l* was taken in 250 ml stoppered conical flask. At appropriate time, samples were withdrawn and filtered with Whatman filter paper. Samples were checked for residual fluoride concentration. Optimization of adsorbent weight was done for both the adsorbents by 0.5 g, 1 g, 1.5 g, 2 g, 2.5 g and 3 g. Influence of temperature on the removal of fluoride was studied at different temperatures of 30 °C, 40 °C, 50 °C and 60 °C. At different RPM, 100, 120, 140, 160, 180 and 200, experiments were conducted for the removal of fluoride.

Optimization of contact time was also studied for defluoridation from water, and equilibrium was attained at 120 minutes. Influence of aqueous phase pH was studied by adjusting pH with 0.1 N HCl and 0.1 N NaOH. Variation of pH was done from 3 to 11 using Elico LI-120 pH meter, keeping concentration 5 mg/*l*, adsorbent 2.5 g, temperature 30 °C, and contact time 120 min. After equilibrium had been attained, the filtrate was analyzed for fluoride concentration. Residual fluoride concentration was analyzed by SPADNS method on UV Spectrophotometer (Shimadzu UV 1800, 240V), as per the standard methods of APHA [52]. Using wavelength (570 nm), the calibration was done for absorbance and concentration.

For accuracy, each experiment was repeated twice for reproducibility of the result with an error of less than 3%. For exact calculation, the original fluoride solution was used for all the experiments. For all calculations, mass balance was accurate.

The amount of fluoride adsorbed per gram of adsorbent was calculated by using the following equation:

$$q_t = \frac{(C_0 - C_t)V}{M} \quad (1)$$

where, q_t is the amount of fluoride adsorbed per gram of adsorbent (mg/g); C_0 is the initial concentration of fluoride (g/*l*) and C_t is the concentration at time t; V is the total volume of suspension (L); M is the mass of adsorbent (g).

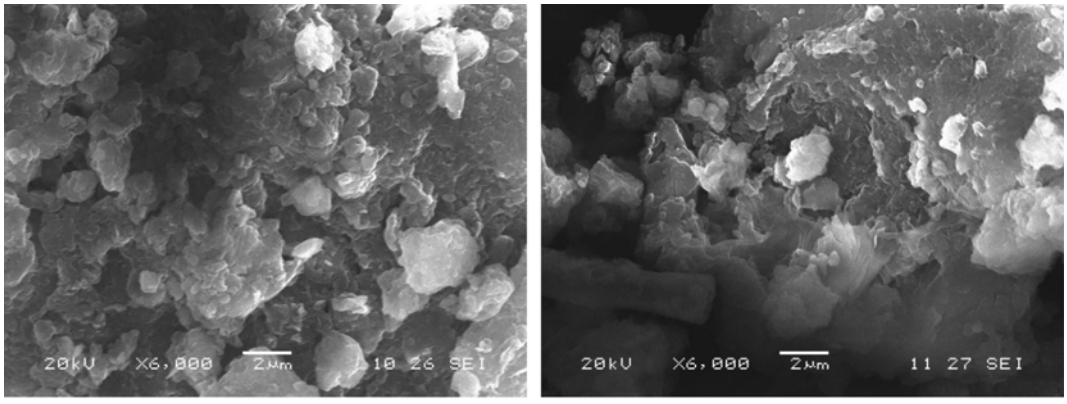

Fig. 1. Scanning electron microscopy of (a) *Azospirillum* biofertilizer. (b) Scanning electron microscopy of lignite.

Table 1. Elemental analysis of *Azospirillum* biofertilizer and Lignite

Sr. no.	Element	Weight % (*Azospirillum* biofertilizer)	Weight% (lignite)
1	C	55	42.52
2	O	40.48	48.16
3	Al	0.66	3.48
4	Si	0.54	2.74
5	S	1.83	1.26
6	Cl	0.13	0.11
7	Ca	0.06	0.24
8	Ti	0.13	0.32
9	Fe	0.82	0.41
10	Cu	0.22	0.20
11	Zr	0.12	0.19
12	Na	-	0.13
13	Mg	-	0.15

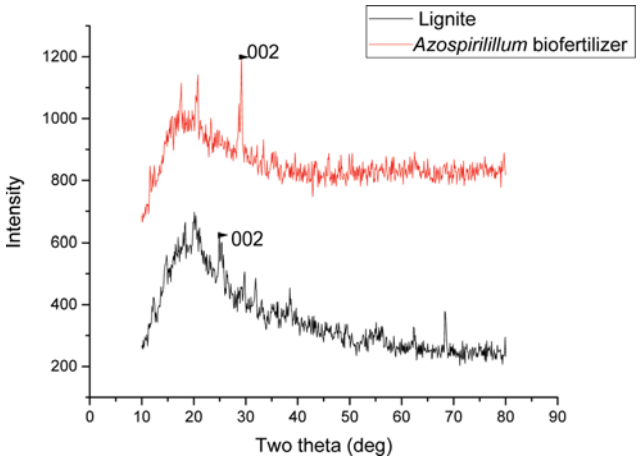

Fig. 2. XRD for *Azospirillum* biofertilizer and lignite.

RESULTS AND DISCUSSION

1. Morphology of *Azospirillum* Biofertilizer and Lignite

Fig. 1(a) and (b) shows the micrographs for *Azospirillum* biofertilizer and lignite respectively. Both the structures are porous. *Azospirillum* is present on the surface of lignite, showing somewhat uniformity of the surface. Elemental analysis showed an increase in elemental carbon content in *Azospirillum* biofertilizer as compared to lignite. O, Al and Si decreased in smaller amounts. *Azospirillum* biofertilizer is an amalgamation of *Azospirillum* and lignite; it shows all the elements present in lignite. Lignite showed more two elements, Na and Mg in small quantity. Utilization of Na and Mg may be done by the bacteria (*Azospirillum*) present in *Azospirillum* biofertilizer.

Fig. 2 shows XRD for *Azospirillum* biofertilizer and lignite. The surrounding intensity showed highly tangled in the form of amorphous carbon in both the adsorbents [53,54]. XRD exhibited somewhat crystalline carbon-like structure, and a band recognized the occurrence of saturated structures such as aliphatic side chains attached to the edge [55-57]. The peak of *Azospirillum* biofertilizer was shifted from 25.2 to 27.0. This may be due to presence *Azospirillum* on the surface.

For lignite the diffraction peak was at 25.20, which clearly showed the presence of 002 plane and the d-spacing value is 1.662. For *Azospirillum* biofertilizer, because of increase in elemental carbon content the diffraction peak was shifted from 25.20 to 27.0. The d-spacing value for the *Azospirillum* biofertilizer for the diffraction peak is 3.02. In both the samples, as compared to other peaks, the 002 peak is more intense and sharp.

2. Effect of Contact Time and Initial Concentration

Effect of contact time on fluoride removal efficiency is shown in Fig. 3(a), (b) for *Azospirillum* biofertilizer and lignite. For 20 minutes the removal efficiency was high and reached the maximum value after 2 hours and thereafter remained constant for *Azospirillum* biofertilizer and lignite. Fluoride removal efficiency showed a decreasing trend as the aqueous phase fluoride concentration was increased from 5 mg/*l* to 25 mg/*l* for *Azospirillum* biofertilizer (76.2% to 41%). Fast removal of fluoride in 20 minutes may be due the penetration of fluoride ions into the pores of the adsorbent. After 20 minutes, the rate of removal stagnated, it increased to 120 minutes where equilibrium was attained.

From Fig. 3(a) and (b) fluoride removal efficiency decreased

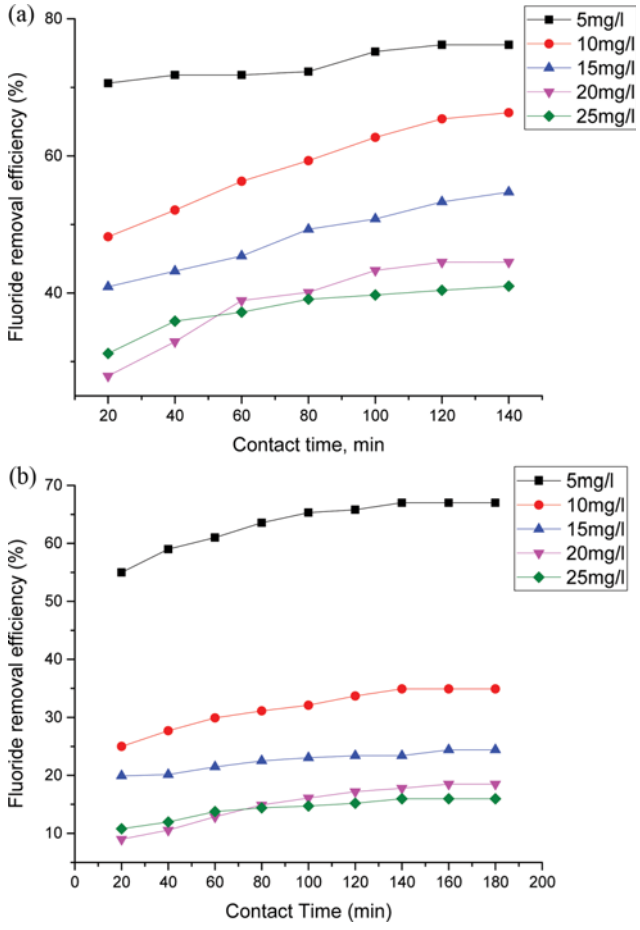

Fig. 3. Effect of contact time on fluoride removal efficiency for (a) *Azospirillum* biofertilizer (b) Lignite.

when initial concentration was increased. This may be due to adsorbent binding capacity which reaches saturation [58]. All the sites of adsorption were used by adsorbent, then the binding capacity of the adsorbent reached saturation. Furthermore, the amount of fluoride adsorbed per unit mass of adsorbent increased with an increase in fluoride concentration as higher numbers of fluoride ions were present [59].

3. Effect of pH

Solution pH is one of the most significant parameters for adsorption of fluoride ions. Fluoride adsorption study was carried out at different pH ranging from 3.0 to 11.0. Fig. 4 represents the effect of pH on fluoride removal. As pH was increased up to 7, fluoride removal efficiency increased gradually. Above pH 7 the fluoride removal efficiency decreased. At low pH there may be increase in electrostatic force between positively charged surface and negative fluoride ions. In acidic pH range fluoride removal was slightly decreased, which may have been due to the formation of weak hydrofluoric acid. In alkaline pH range, the removal of fluoride was found to be decreased, maybe due to the competition with the hydroxyl ions with the fluoride ions for adsorption as fluoride and hydroxyl ions are having similar charge and ionic radius [60]. For *Azospirillum* biofertilizer and lignite the maximum removal efficiency was obtained at neutral pH.

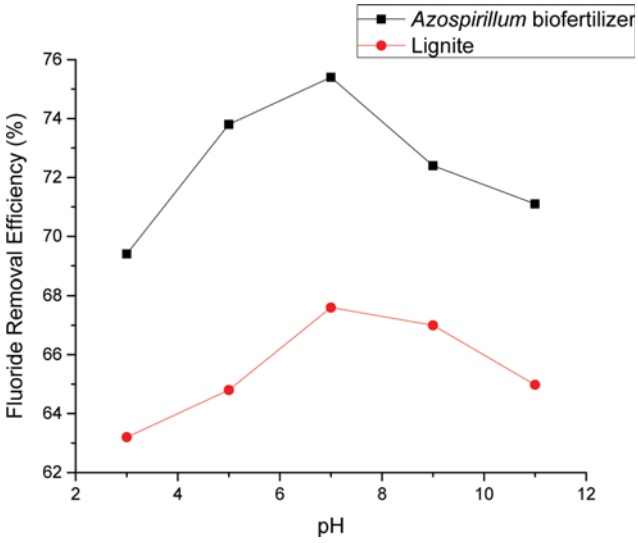

Fig. 4. Effect of pH on fluoride removal efficiency for *Azospirillum* biofertilizer and lignite.

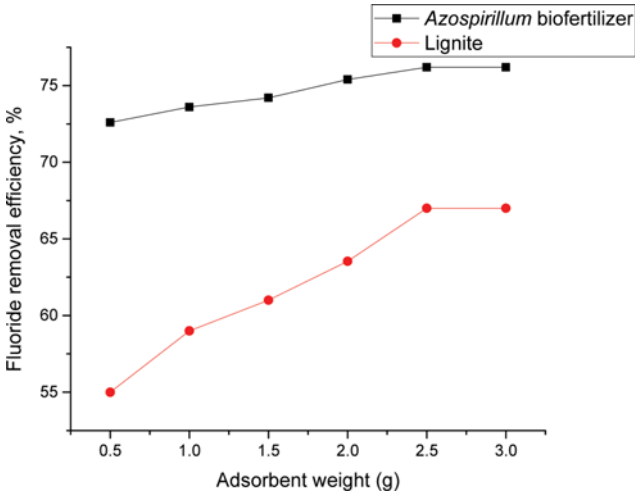

Fig. 5. Effect of adsorbent dose on fluoride removal efficiency for *Azospirillum* biofertilizer and lignite.

4. Effect of Adsorbent Dose

Fig. 5 shows the effect of adsorbent dose on fluoride removal. Experiments were conducted for 5 mg/*l* fluoride concentration, contact time of 120 minute, 100 rpm, pH 7 and temperature 30 °C. Fluoride removal efficiency was increased as adsorbent dose was increased. Maximum removal efficiency was observed for 2.5 g adsorbent dose. Fluoride removal efficiency increases at first because of large number of adsorption sites available but later on the sites get occupied by fluoride ions. As the adsorbent dose was increased, the adsorption sites may have gotten saturated by adsorption reaction, and due to particle particle reaction, the particles may agglomerate, causing a decrease in surface area resulting in increased diffusion path [61].

5. Effect of Temperature

To study the effect of temperature, experiments were conducted at different temperatures as shown in Fig. 6. Fluoride removal effi-

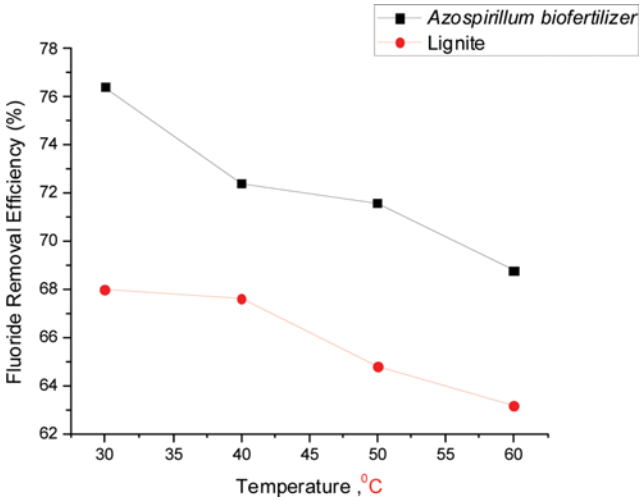

Fig. 6. Effect of temperature on fluoride removal efficiency for *Azospirillum* biofertilizer and lignite.

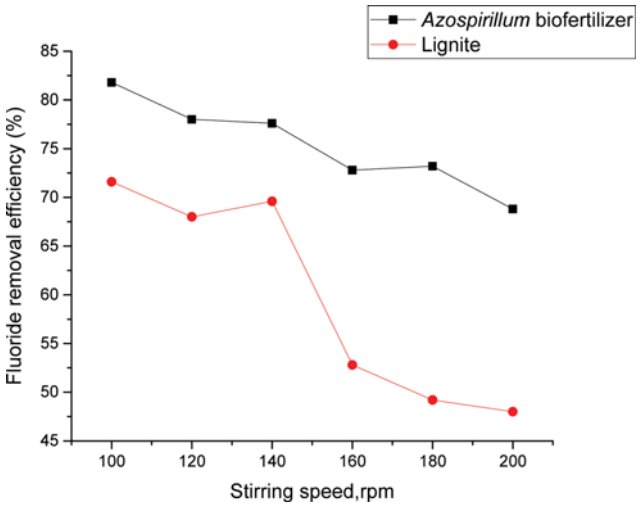

Fig. 7. Effect of rpm on fluoride removal efficiency for *Azospirillum* biofertilizer and lignite.

ciency decreased as temperature was increased. The decrease in fluoride removal efficiency may be due to the decrease in the number of active sites of the adsorbent and resulting in deterioration of adsorptive forces between surface of *Azospirillum* biofertilizer and fluoride ions. Same tendency was seen for lignite. Effect of temperature shows the surface is heterogeneous and adsorption is exothermic [62]. Maximum removal was at 30 °C.

6. Effect of rpm

Adsorption experiments were conducted at six different rpm (100, 120, 140, 160, 180 and 200 rpm). Increase in rpm decreased the fluoride removal efficiency, which is shown in Fig. 7. At higher rpm more centrifugal force is created, and due to this the bonding between adsorbent and adsorbate decreased, which may be the cause of decrease in removal efficiency. At 100 rpm, maximum fluoride removal efficiency was observed. Experiments were conducted without stirring, but only 17% fluoride removal efficiency was observed.

7. Probable Adsorption Mechanism

It is well known that microorganisms have high affinity towards various non-metals and metals [63,64]. Microbes are small, which provides high surface area. They offer large contact area for interaction with essentials in the environment [65]. Immobilization of microorganisms on carrier material increases the contact area and the cell count. Microorganisms have capability to bear and decrease the fluoride quantity. Specific bacterial cells possess exceptional property of concentrating fluoride inside their cells [66,67]. Many bacteria and plants exude high affinity anion binding compounds. These are called ionphores. Ionophores form a complex with specific types of anions and assist to move across cell membrane. The ionophore-anion complex may be absorbed back into the cell for consumption [68,69]. Defluoridation may occur due to the combined effect of two phenomena. The first one is due to formation of ionosphere-anion complex formed by *Azospirillum* bacteria and absorption of fluoride inside the cell. The second one is the adsorption of fluoride on lignite on active sites. Increased efficiency may be due to the combined effect of these two phenomena. The probable fluoride removal mechanism can be represented schematically as shown below.

Additional work is required on the binding mechanism, which will explain the transport of complex inside the cell.

ADSORPTION KINETICS

For the feasibility of large scale operation and to get practical data about efficiency of adsorption, kinetic study is essential. The

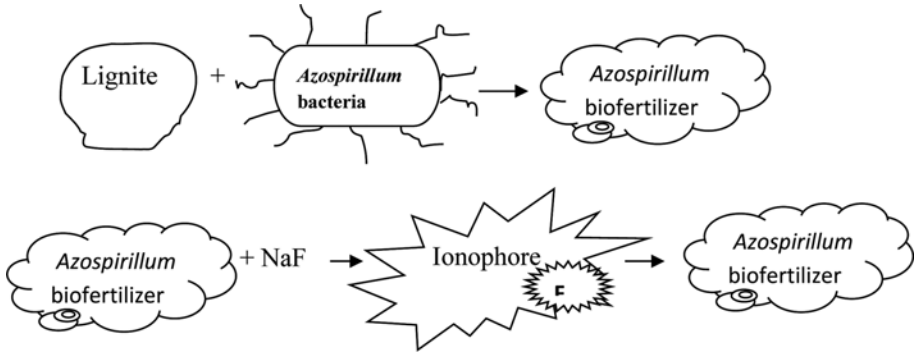

Fig. 8. Probable mechanism of fluoride removal.

experimental data were tested for different kinetic models such as intraparticle diffusion model [70], pseudo-first-order model [71] and pseudo-second-order model [72].

1. Intraparticle Diffusion Model

The linear equation for intraparticle diffusion is represented as:

$$q_t = k_p t^{0.5} \quad (2)$$

The intraparticle diffusion rate constant is k_p (mg/g $min^{-0.5}$), q_t is the fraction of fluoride removed (mg/g), and t is contact time (min). For the intraparticle diffusion model the basic assumption is only that intraparticle diffusion was the rate controlling and film diffusion was negligible. Intraparticle diffusion model applicability suggests that the adsorption process involves both boundary layer and intraparticle diffusion [73-75]. A plot of q_t versus $t_{0.5}$ for *Azospirillum* biofertilizer shows initial curved position and final linear position, which is shown in Fig. 8(a). The first portion suggests boundary layer diffusion, while another stage which is linear suggests the intraparticle diffusion effect. For lignite as shown in Fig. 8(b) also the first position is curved and then it is a straight line. This suggests that intraparticle was not only the rate controlling step [76].

For *Azospirillum* biofertilizer and lignite, rate parameter k_p is the slope of linear portion which is a characteristic of the rate of adsorption in intraparticle diffusion controlling region and is reported in Table 2.

Table 2. Summary of adsorption data evaluated by different kinetic models for *Azospirillum* biofertilizer and lignite

Initial fluoride concentration, mg/*l*	Rate constant	R^2
Intraparticle diffusion model for *Azospirillum* biofertilizer		
5	0.001 mg/g $min^{0.5}$	0.914
10	0.001 mg/g $min^{0.5}$	0.993
15	0.011 mg/g $min^{0.5}$	0.979
20	0.017 mg/g $min^{0.5}$	0.943
25	0.011 mg/g $min^{0.5}$	0.91
Intraparticle diffusion model for lignite		
5	0.003 mg/g $min^{0.5}$	0.966
10	0.005 mg/g $min^{0.5}$	0.988
15	0.003 mg/g $min^{0.5}$	0.958
20	0.009 mg/g $min^{0.5}$	0.986
25	0.006 mg/g $min^{0.5}$	0.964
Pseudo-first-order kinetic model for *Azospirillum* biofertilizer		
5	0.018 min^{-1}	0.735
10	0.021 min^{-1}	0.965
15	0.021 min^{-1}	0.915
20	0.029 min^{-1}	0.96
25	0.026 min^{-1}	0.988
Pseudo-first-order kinetic model for lignite		
5	0.023 min^{-1}	0.983
10	0.019 min^{-1}	0.953
15	0.014 min^{-1}	0.960
20	0.021 min^{-1}	0.976
25	0.019 min^{-1}	0.986
Pseudo-second-order kinetic model for biofertilizer		
5	1.81098 g/mg min	0.999
10	0.21697 g/mg min	0.996
15	0.1294 g/mg min	0.996
20	0.125 g/mg min	0.998
25	0.0271 g/mg min	0.999
Pseudo-second-order kinetic model for lignite		
5	0.9963 g/mg min	0.997
10	0.7142 g/mg min	0.999
15	0.754 g/mg min	0.998
20	0.133 g/mg min	0.989
25	0.3560 g/mg min	0.997

2. Pseudo-first and Second-order Models

The kinetic process described by each equation is different. To follow the first-order kinetics the linear equation is:

$$\ln(q_e - q_t) = \ln q_e - k_1 t \quad (3)$$

If the adsorption process follows a pseudo-second-order kinetics, the reaction rate equation is:

$$\frac{dq_t}{dt} = k_2(q_e - q_t)^2 \quad (4)$$

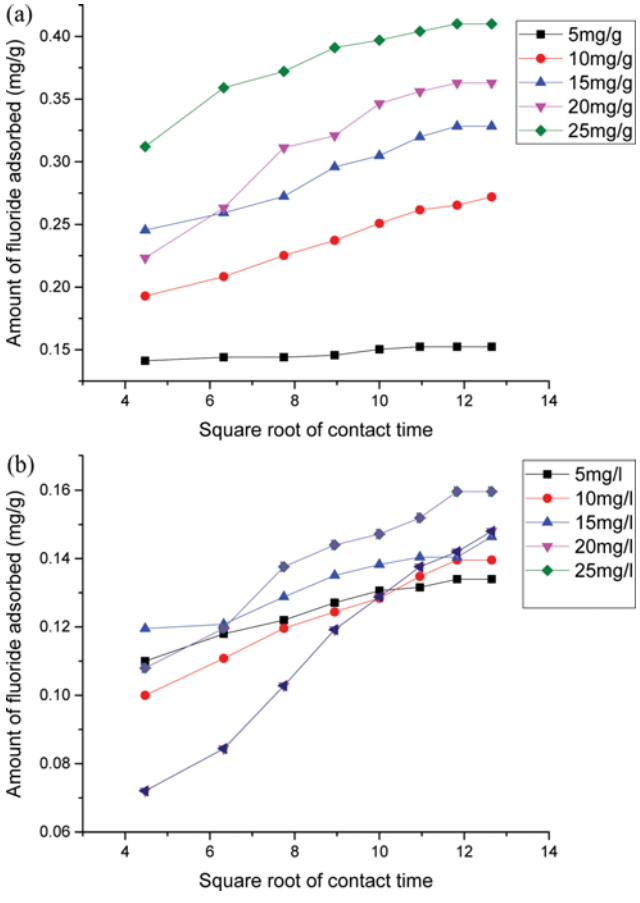

Fig. 9. Intraparticle diffusion model for (a) *Azospirillum* biofertilizer and (b) lignite [temperature 30 °C; stirring speed: 100 rpm; adsorbent 2.5 g; pH 7.0].

where q_e is the concentration of fluoride at equilibrium, q_t is the concentration of fluoride at contact time t (min). k_1 (min^{-1}) and k_2 (g/mg min) are the rate constant for pseudo-first-order and pseudo-second-order respectively. If the adsorption process follows pseudo-first-order kinetics a plot of ln ($q_e - q_t$) versus t would confirm by a straight line. If the adsorption system follows a pseudo-second-order kinetics a plot of t/q_t versus t is linear.

Fig. 9(a) and (b) shows the plot for pseudo-first-order model for *Azospirillum* biofertilizer and lignite, respectively. The values of kinetic parameters are in Table 2.

The pseudo-second-order showed the best fit among all three kinetic models. All the correlation coefficients were 0.99, shown in Table 2. Next good fit for the experimental data was intraparticle diffusion model (>0.91) followed by pseudo-first-order kinetic model (>0.73). The pseudo-first-order correlation coefficients were in between 0.735 to 0.98, which suggests its limited applicability. For pseudo-second-order model the rate constant decreases with increase in concentration. There was slight change in the rate constants of intraparticle diffusion when concentration was increased. This reveals that boundary layer diffusion decreases with increase in concentration [77,78]. From the kinetic data it can be generalized that the pseudo-second-order kinetic model is a generalized model for adsorption process study.

3. Adsorption Isotherm

Analysis of equilibrium data is important and provides the relationship between amount of fluoride adsorbed on the surface and concentration of the solution at equilibrium. The Langmuir, Freundlich and Temkin isotherms were studied for removal of fluoride and initial concentration for *Azospirillum* biofertilizer and lignite. The linear from of Langmuir isotherm is:

$$\frac{C_{eq}}{q_{eq}} = \frac{1}{k_a Q_m} + \frac{C_{eq}}{Q_m} \tag{5}$$

where Q_m (mg/g) is the maximum adsorption capacity of the adsorbent and k_a (1/mg) is the Langmuir constant related to binding sites. From the linear isotherm of Fig. 11(a) and (b) the kinetic data is listed in Table 3.

Feasibility of Langmuir isotherm was expressed by separation factor or equilibrium parameter defined by Eq. (6) [79].

$$R_L = 1/1 + k_a C_0 \tag{6}$$

where C_0 is the initial concentration and R_L is the separation fac-

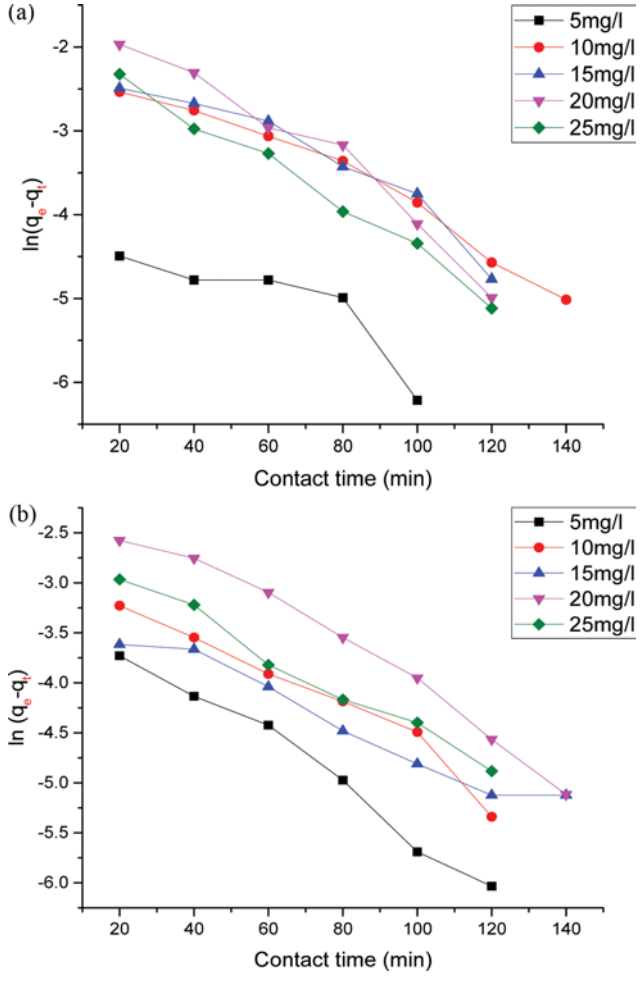

Fig. 10. Pseudo-first-order model for (a) *Azospirillum* biofertilizer (b) lignite.

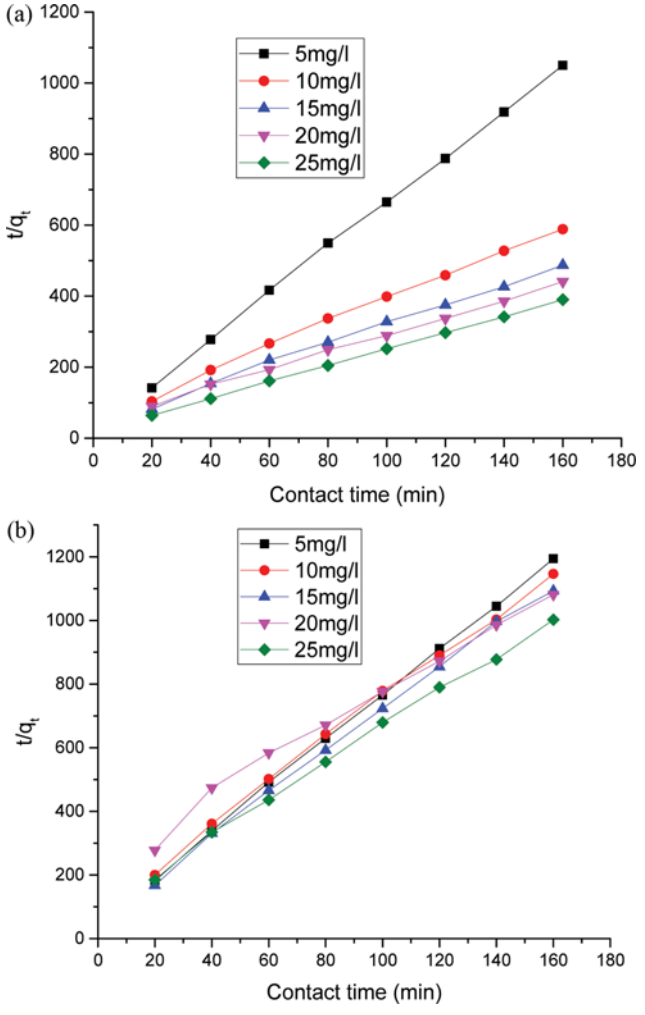

Fig. 11. Pseudo-second-order model for (a) *Azospirillum* biofertilizer (b) lignite.

tor. R_L values determine the favorability of the adsorption process. R_L>1 is unfavorable, R_L=1 linear, R_L values 0<R_L<1 are favorable and R_L=0 is reversible. For fluoride adsorption the values of R_L obtained are between 0.091 to 0.334, suggesting that the adsorption of fluoride on *Azospirillum* biofertilizer was favorable. For Lignite also R_L obtained is between 0.134 to 0.030, indicating adsorption of fluoride on lignite was favorable.

Freundlich isotherm is used to study the processes involved in heterogeneous surfaces. The linearized form of the equation is as follows:

$$\mathrm{Log}(q_{eq}) = \frac{1}{n}\log(C_{eq}) + \log(k_f) \quad (7)$$

where, k_f is the Freundlich constant (mg/g) and 1/n denotes the adsorption intensity (*l*/mg).

From the plot Fig. 12(a) and (b) values of Freundlich constants are given in Table 3.

Temkin isotherm is the initial reported isotherm which assumes that the heat of adsorption decreases linearly with increasing coverage. The linear equation for Temkin isotherm is shown by Eq. (8).

Table 3. Isotherm parameters and correlation coefficients for adsorption of fluoride for *Azospirillum* biofertilizer

Isotherm	Parameters	Values	Correlation coefficient
Langmuir	Q_m (mg/g)	0.45598	0.995
	k_a (*l*/mg)	0.398	
Freundlich	n (g/*l*)	2.6737	0.955
	k_f ((*l*/mg)$^{1/n}$)	2.24	
Temkin	B_1 (mg/g)	0.097	0.987
	A (L/mg)	4.36	

Table 4. Isotherm parameters and correlation coefficients for adsorption of fluoride for lignite

Isotherm	Parameters	Values	Correlation coefficient
Langmuir	Q_m (mg/g)	0.161	0.995
	k_a (*l*/mg)	1.283	
Freundlich	n (g/*l*)	16.94	0.829
	k_f ((*l*/mg)$^{1/n}$)	2.44	
Temkin	B_1 (mg/g)	0.008	0.807
	A (L/mg)	4.89	

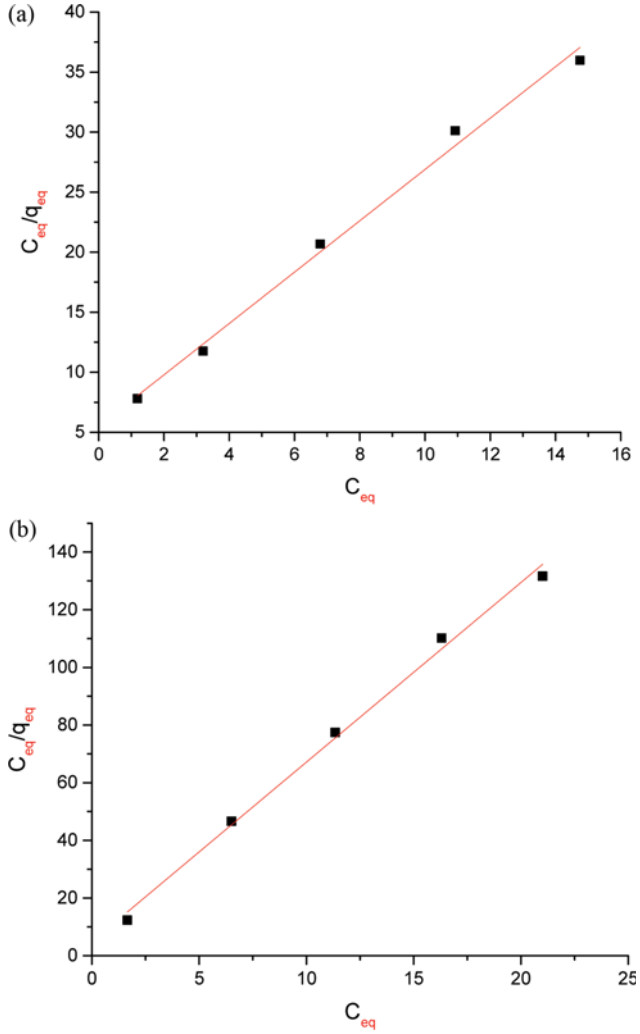

Fig. 12. Langmuir isotherm plot for (a) *Azospirillum* biofertilizer (b) lignite.

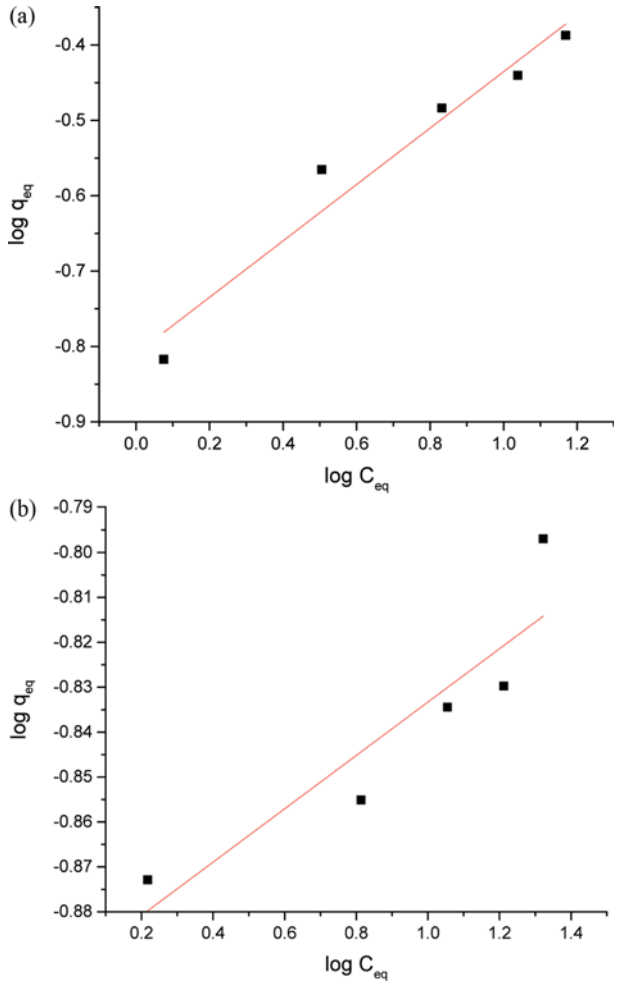

Fig. 13. Freundlich isotherm plot for (a) *Azospirillum* biofertilizer (b) lignite.

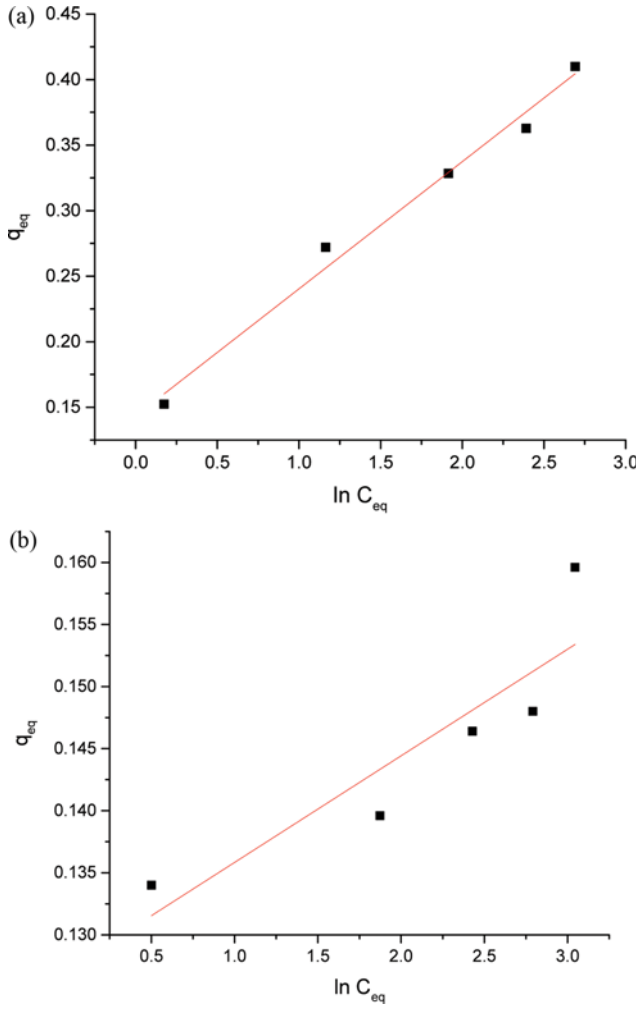

Fig. 14. Temkin isotherm plot for (a) *Azospirillum* biofertilizer (b) lignite.

$$q_e = B_1 \ln A + B_1 \ln C_e \quad (8)$$

Fig. 13 represents Temkin isotherm for Biofertilizer (a) and Lignite (b).

Langmuir isotherm was the best fit, having highest correlation coefficient as 0.995. These factors confirmed that all present sites are similar and there is no migration from one place to another in a place. The adsorption of fluoride ions had affinity towards surface functional groups [80].

LEACHABILITY OF THE ADSORBENT

As maximum removal of fluoride was obtained at neutral condition, so the leachability was also observed at neutral condition. Used adsorbent and 500 ml distilled water were mixed and kept for stirring. Total contact time was 180 minutes. The solution was filtered. Filtrate and adsorbent were analyzed for fluoride content. Results of the analysis showed that fluoride was not present on the adsorbent, but in filtrate 10% of the fluoride was leached. The rest of the fluoride may be used by the bacteria as per the proposed mechanism. After the use of *Azospirillum* biofertilizer as fluoride removal, the adsorbent was analyzed for fluoride content. The analysis showed absence of fluoride on the adsorbent. So as a biofertilizer it is safe after its use as fluoride remover.

FIELD STUDIES

Water samples were collected from the well from the sugarcane farm near Karad district, Maharashtra, India. The initial concentration of fluoride was 9.62 mg/*l*. It was treated by using *Azospirillum* biofertilizer and lignite. Optimized parameters like 2.5 g of adsorbent dose, 100 rpm and at pH 7 the water sample from farm was treated for 120 minutes at 30 °C. By the use of *Azospirillum* biofertilizer the fluoride concentration was reduced to 2.01 mg/*l* (79.1%) and by using lignite it was reduced to 4.09 mg/*l* (57.58%).

CONCLUSIONS

WE studied *Azospirillum* biofertilizer and lignite for removal of fluoride. Batch adsorption experiments were performed and showed good fluoride removal efficiency. For 5 mg/*l* concentration the fluoride removal efficiency was 72.6% for contact time of 120 minutes by using *Azospirillum* biofertilizer, and for Lignite it was 67% for 120 minutes contact time. Biofertilizer showed more removal of fluoride than Lignite. Pseudo-first-order kinetics was suitable for the kinetic data. Langmuir isotherm was found to be good fit to the kinetic data of adsorption. From all the results, *Azospirillum* biofertilizer can be used to serve both for removal of fluoride from water and as fertilizer which will increase the crop production.

ACKNOWLEDGEMENTS

The authors thank Professors Anand Kulkarni and Prashant Chaudhari from Bharati Vidyapeeth University College of Engineering, Pune for their suggestions, comments and helpful discussions.

REFERENCES

1. V. Tomar and V. D. Kumar, *Chem. Cent. J.*, **7**, 2 (2013).
2. WHO (World Health Organization) Guidelines for drinking water quality. World Health Organization, Geneva (2004).
3. M. Mahramanlioglu, I. Kizilcikli and I. O. Bicer, *J. Fluorine Chem.*, **115**, 41 (2002).
4. A. V. Jamode, V. S. Sapkal and V. S. Jamode, *J. Indian Inst. Sci.*, **84**, 163 (2004).
5. C. Gonzales, H. Hotokezaka, EI. Karadeniz, T. Miyazaki, E. Kobayashi, M. Darendeliler and N. Yoshida, *Am. J. Ortho Dentofacial Orthop.*, **139**, 196 (2011).
6. I. Solangi, S. Memon and M. Bhanger, *J. Hazard Mater.*, **171**, 815 (2009).
7. X. Fan, D. J. Parker and M. D. Smith, *Water Res.*, **37**, 4929 (2003).
8. S. Meenakshi and N. Viswanathan, *J. Colloid Interface Sci.*, **308**, 38 (2007).
9. M. Onyango, Y. Kojima, O. Aovi, E. Bernardo and H. Matsuda, *J. Colloid Interface Sci.*, **279**, 341 (2004).

10. S. S. Tripathy, J. L. Bersillon and K. Gopal, *Sep. Purif. Technol.*, **50**, 310 (2006).
11. M. Hichour, F. Persin, J. Molenat, J. Sandeaux and C. Gavach, *Desalination*, **122**, 53 (1999).
12. W. B. Apambire, D. R. Boyle and F. A. Michel, *Environ. Geol.*, **33**, 13 (1997).
13. S. Ghorai and K. K. Pant, *Sep. Purif. Technol.*, **42**, 265 (2005).
14. M. M. Shihabudheen, S. Shukla, L. Philip and I. M. Nambi, *Chem. Eng. J.*, **140**, 183 (2008).
15. S. S. Tripathy, J. L. Bersillon and K.Gopal, *Sep. Purif. Technol.*, **50**, 310 (2006).
16. P. I. Ndiaye, P. Moulin, L. Dominguez, J. C. Millet and F. Charbit, *Desalination*, **173**, 25 (2005).
17. M. Tahaikt, R. El Habbani, A. Ait Haddou, I. Achary, Z. Amor, M. Taky, A. Alami, A. Boughriba, M. Hafsi and A. Elmidaoui, *Desalination*, **212**, 46 (2007).
18. C. J. Huang and J. C. Liu, *Water Res.*, **33**, 3403 (1999).
19. M. Yang, Y. Zhang, B. Shao, R. Qi and H. Myoga, *J. Environ. Eng.*, **127**, 902 (2001).
20. M. Mohapatra, S. Anand, B. K. Mishra, D. E. Giles and P. Singh, *J. Environ. Manage.*, **91**, 67 (2009).
21. X. M. Wu, Y. Zhang, X. M. Dou and M. Yang, *Chemosphere*, **69**, 1758 (2007).
22. L. A. Khandare, P. UdayKumar, G. Shankar, K. Venkaiah and N. Laxmaiah, *Nutrition.*, **20**, 433 (2004).
23. T. Ramachandra Murthy, D. A. Jeyakar, R. Chellaraj, T. Edison Raja, R. Venkatachalam, Sangeetha and C. Sivaraj, *IJEP*, **239**, 317 (2003).
24. L. U. Simha, B. Panigrahy and S. V. Ramakrishna, *IJEP*, **22**, 506 (2002).
25. B. Jamode, S. Chandak and M. Rao, *Pollut. Res.*, **23**, 239 (2004).
26. S. V. Mohan, N. C. Rao, K. K. Prasad and J. Karthikeyan, *Waste Manage.*, **22**, 575 (2002).
27. P. Mariappan, V. Yegnaraman and T. Vasudevan, *IJEP*, **22**, 154 (2000).
28. R. S. Prakasam, P. L. ChandraReddy, A. Manisha and S. V. Ramakrishna, *IJEP*, **19**, 119 (1998).
29. S. V. Mohan and J. Karthikeyan, *Toxicol. Environ. Chem.*, **74**, 147 (2000).
30. S. V. Mohan, Y. V. Bhaskar and J. Karthikeyan, *Int. J. Environ. Pollut.*, **21**, 211 (2003).
31. N. K. Mondal, R. Bhaumik, T. Baur, B. Das, P. Roy and J. K. Datta, *Chem. Sci. Trans.*, **1**, 239 (2012).
32. S. V. Mohan, S. V. Ramanaiah, B. Rajkumar and P. N. Sarma, *J. Hazard. Mater.*, **141**, 465 (2007).
33. S. V. Ramanaiah, S. V. Mohan and P. N. Sarma, *Ecological Engineering*, **31**, 47 (2007).
34. S. Mukherjee, V. Yadav, M. Mondal, S. Banerjee and G. Halder, *Appl. Water Sci.*, **7**, 1923 (2017).
35. S. Chouhan, U. Tuteja and J. S. Flora, *Appl. Biochem. Microbiol.*, **48**, 43 (2012).
36. M. Bhatnagar, A. Bhatnagar and S. Jha, *Biotechnol. Lett.*, **24**, 1079 (2002).
37. P. Miretzky, C. Munoz and A. Carrillo-Chavez, *Environ. Chem.*, **5**, 68 (2008).
38. S. Sinha, K. Pandey, D. Mohan and K. P. Singh, *Ind. Eng. Chem. Res.*, **42**, 6911 (2003).
39. A. K. M. Arnesen, *Plant and Soil*, **191**, 13 (1997).
40. G. W. Miller, *Fluoride*, **26**, 3 (1993).
41. R. E. Brewer, M. J. Garber, F. B. Guillemet and F. H. Sutherland, *Proceedings of the American Society of Horticultural Science*, **91**, 150 (1967).
42. J. R. Istas and G. Alaerts, *Revue de l' Agriculture*, **27**, 487 (1974).
43. J. S. Jacobson, L. H. Weinstein, D. C. McCune and A. E. Hitchcock, *J. Air Pollut Control Assoc.*, **16**, 412 (1996).
44. S. K. Jha, A. K. Nayak and Y. K. Sharma, *Eco Toxicology and Environmental Safety*, **74**, 940 (2011).
45. R. D. Souza, A. Ambrosini and L. M. P. Passaglia, *Genet Mol. Biol.*, **38**, 401 (2015).
46. B. Volesky and Z. R. Holan, *Biotechnol. Prog.*, **11**, 235 (1995).
47. H. A. Smith, S. L. Swaney, T. D. Parks, E. A. Wernsman and W. G. Dougherty, *Plant Cell*, **6**, 1441 (1994).
48. T. J. Beveridge, *J. Nucl. Radiochem. Sci.*, **6**, 7 (2005).
49. N. Chubar, T. Behrends and P. V. Cappellen, *Colloids Surf., B: Biointerfaces*, **65**, 126 (2008).
50. J. Richard, R. Petit and R.Taber, *Phytopathology*, **74**, 1167 (1984).
51. T. A. M. Msagati, B. B. Mamba, V. Sivasankar and K. Omine, *Appl. Surf. Sci.*, **301**, 235 (2014).
52. SPANDAN -APHA, Standard methods for examination of water and waste water, 20th Ed., Americal Public Health Association, Washington, DC (1998).
53. H. Takagi, K. Maruyama, N. Yoshizova, Y. Yamada and Y. Sato, *Fuel*, **83**, 2427 (2004).
54. M. Sudip and M. Pinaki, *Curr. Sci.*, **91**, 337 (2006).
55. P. H. Klug and L. E. Alexander, Wiley, New York (1974).
56. O. O. Sanibare, H. Tobias and F. F. Stephen, *Energy*, **35**, 5347 (2010).
57. L. Xiajiang, H. Juninchiro and L. ChunZhu, *Fuel*, **85**, 1700 (2006).
58. S. K. Swain, T. Patnaik, V. K. Singh, U. Jha, R. K. Patel and R. K. Dey, *Chem. Eng. J.*, **171**, 1218 (2011).
59. M. Karthikeyan, K. K. SatheeshKumar and K. P. Elango, *J. Fluorine Chem.*, **130**, 894 (2009).
60. S. Gao, J. Cui and Z. Wei, *J. Fluorine Chem.*, **130**, 1035 (2009).
61. A. Shukla J. Das and K. Parida, *J. Hazard. Mater.*, **95**, 137 (2002).
62. D. P. Das, J. Das and K. Parida, *J. Colloid Interface Sci.*, **261**, 213 (2003).
63. J. J. Harrison, M. Rabie, R. J. Turner, E. A. Badry, K. M. Sproule and H. Ceri, *FEMS. Microbiol. Ecol*, **55**, 479 (2006).
64. M. Pas, R. Milacic, K. Dralar, N. Pollak and P. Raspor, *Biometals*, **17**, 25 (2004).
65. M. Ledin, *Earth Sci. Rev.*, **51**, 1 (2000).
66. D. Brighton and W. A. McDougall, *J. Dent. Res.*, **56**, 1185 (1977).
67. D. Brighton and G. Colman, *J. Dent. Res.*, **55**, 875 (1976).
68. K. Dolowy, *Cell. Biol. Mol. Lett.*, **6**, 343 (2001).
69. K. S. Kim, C. Cui and S. J. Cho, *J. Phys. Chem. B.*, **102**, 461 (1998).
70. J. Walter, J. Weber and J. C. Morris, *J. Sanitary Eng.*, **89**, 31 (1963).
71. S. Lagergren, Zurtheorie der sogenannten adsorption gelosterstoffe, Kungliga Svenska, Vetenskapsakademiens Handlingar, **24**, 1 (1898).
72. Y. S. Ho and G. Mckay, *Proc. Biochem.*, **34**, 451 (1999).
73. S. V. Mohan and J. Karthikeyan, *Environ. Pollut.*, **1-2**, 183 (1997).
74. S. V. Mohan, N. C. Rao and J. Karthikeyan *J. Hazard. Mater.*, **90**, 189 (2002).

75. M. Yalcin, A. Gurses, C. Dogar and M. Sozbilir, *Adsorption*, **10**, 339 (2004).
76. M. Sarkar, P. K. Acharya and B. Bhattacharya, *J. Colloid Interface Sci.*, **266**, 28 (2003).
77. V. S. Mane and P. V. V. Babu, *Desalination*, **273**, 321 (2011).
78. Y. Liu, J. Wang, Y. Zheng and A. Wang, *Chem. Eng. J.*, **184**, 248 (2012).
79. W. Weber and R. K. Chakraborti, *J. Am. Inst. Chem. Eng.*, **20**, 228 (1974).
80. T. J. Cao, J. Lin, F. Fang, M. Zhang and Z. Hu, *Bioresour. Technol.*, **163**, 199 (2014).